

BRNO UNIVERSITY OF TECHNOLOGY

Faculty of Mechanical Engineering  
Institute of Machine and Industrial Design

Ing. Pavel Čípek

**THE EFFECT OF SYNOVIAL FLUID  
CONSTITUENTS ON FRICTION AND  
LUBRICATION OF ARTICULAR CARTILAGE**

**VLIV SLOŽEK SYNOVIÁLNÍ KAPALINY NA TŘENÍ  
A MAZÁNÍ KLOUBNÍ CHRUPAVKY**

*Shortened version of PhD Thesis*

Branch: Design and Process Engineering

Supervisor: doc. Ing. Martin Vrbka, Ph.D.

**Keywords:**

Biotribology, cartilage, reciprocating tribometer, friction, lubrication, fluorescence microscopy

**Klíčová slova:**

Biotribologie, chrupavka, reciproční tribometer, tření, mazání, fluorescenční mikroskopie

**Místo uložení práce:**

Oddělení pro vědu a výzkum FSI VUT v Brně.

# CONTENTS

<b>1</b>	<b>INTRODUCTION</b>	<b>4</b>
<b>2</b>	<b>STATE OF ART</b>	<b>5</b>
2.1	Biotribology of synovial joint	5
<b>3</b>	<b>ANALYSIS AND CONCLUSION OF LITERATURE REVIEW</b>	<b>15</b>
<b>4</b>	<b>AIM OF THESIS</b>	<b>17</b>
4.1	Scientific questions	17
4.2	Hypotheses	17
4.3	Thesis layout	18
<b>5</b>	<b>MATERIALS AND METHODS</b>	<b>19</b>
5.1	Fluoresce microscopy – visualization method	20
5.2	Specimens and conditions	21
5.2.1	AC specimens	21
5.2.2	Lubricants	21
5.2.3	Experimental conditions	22
5.3	Methodology and experimental design	22
<b>6</b>	<b>RESULTS AND DISCUSSION</b>	<b>26</b>
6.1	Lubricating film formation in the model of synovial joint	27
<b>7</b>	<b>CONCLUSIONS</b>	<b>30</b>
	<b>REFERENCES</b>	<b>32</b>
	<b>AUTHOR'S PUBLICATIONS</b>	<b>36</b>
	<b>CURRICULUM VITAE</b>	<b>38</b>
	<b>ABSTRACT</b>	<b>39</b>

# 1 INTRODUCTION

Despite the fact that the human society takes it for granted, the natural human joint can be affected by a variety of diseases that can damage it and limit its function [1]. The proper function of human natural musculoskeletal system requires, from a tribological point of view, well lubricated contact surfaces of natural joints, which is closely related to a very low friction coefficient (CoF) and low wear on cartilaginous surfaces of the natural joint. The diseases disrupt the tribological environment in the joint, and the unique properties deteriorate. There are many types of joint diseases (arthrosis, arthritis, osteoarthritis, etc.) and each of them affects and degrades the natural joint differently. The natural joint is gradually damaged and, if a professional medical intervention is not performed, the joint can be damaged to the degree where movement is not possible. The disease of unfunctional natural joint is almost healed with total replacement, when the joint is replaced for the artificial one [2]. The joint replacement fully compensates the natural joint but its lifetime is limited. When the lifetime of the replacement ends, the artificial joint is too damaged, and it needs to be replaced with a new one. In this case, the correct function of human movement system is preserved; nevertheless, the artificial joints have an average lifetime of 10 – 20 years [3]. When the disease and damage of the natural joint occurs in young patients, the artificial joint will need to be replaced more than once. The human body does not have the ability to handle the artificial joint reoperation repeatedly, because of bone degradation, and the surgery also has an impact on the overall health condition of the patient [4]. Therefore, if the patient's natural joint is damaged at young age, these patients, in old age, remain with an incurable artificial joint, and their movement system is unfunctional.

Due to the acute problems with longevity of endoprosthesis, scientists have come up with non-invasive treatment of diseased natural joints. The supplement is a gel-like liquid, based on hyaluronic acid (HA) and it is injected into the joint gap [4]. Its primary function is to restart the lubrication processes in the synovial joint, which can improve the protection of the cartilage surface; Ideally, the disease progression is stopped, or there is at least a slowdown in the process of joint degradation. The general effort of viscosupplementation is to postpone the necessity of the surgery of damaged natural joint for as long as possible [4]. The supplement therapy is usually effective, unfortunately this is not guaranteed in every patient; therefore, it is obvious that the principles of the viscosupplementation function have not yet been fully understood [5]. For better understanding of viscosupplementation principles, a full description of the lubricating processes in the natural synovial joint is necessary. The description of lubricating film formation in the cartilage contact (a model of natural synovial joint) holds a key role in understanding the viscosupplementation function; therefore, a full understanding of this issue can help us to develop an effective supplement for the whole spectrum of patients with diseased joints.

## 2 STATE OF ART

Even though tribology is relatively young scientific field, the tribology of nature synovial joint (NSJ) is a field with abundant number of publications. The first publication appeared at the beginning of the last century. This research field, dealing with tribology of biological components, has to deal with impossibility of simulation of real situations. The real biological subject has to be replaced with model situation, in this case a replacement of the real human synovial joint with a model of synovial joint, in order to simulate the contact of synovial joint. The experimental models vary depending on the focus of the experimental task, however one half of the contact pair of the experimental model is always an articular cartilage (AC) sample removed from an animal joint.

### 2.1 Biotribology of synovial joint

Most works published so far, are experimental tasks focused on friction detection. The tasks are focused on determining the CoF in different contact pairs, types of motion, lubricants, etc. The whole portfolio of the “friction” works forms a comprehensive state of knowledge, summarizing the friction behaviour of the AC under different conditions. All experiments show unique character of CoF trend, and very low value of CoF, usually ranging in hundredths. Extensive review study overviewing CoF values was published by Jarrett M. L. et al. [6]. The values of CoF vary depending on used material combinations, lubricant, operational conditions or used experimental device. The choice of experimental lubricant has great impact on the value of CoF in the AC contact. Many authors found the best tribological properties while using synovial fluid as the experimental lubricant [7].

The CoF is affected not only by load, lubricant or material combination of testing samples, but also by region on the AC surface from which the sample is removed. Dependency between values of CoF and region from which the sample is removed is described for example in study from Chan S. M. T. et al. [8]. The study used samples removed from knee joint of calves. The samples were removed from two places; medial anterior (M1) and posterior (M4). The Position M1 represents region with relatively high contact pressure in vivo and M4 represents region with relatively low contact pressure in vivo. The removed samples had a diameter of 4 mm. As follows from previous literature [9], these regions are characterized by different mechanical properties, which study [8] put into context with CoF level. The phosphate buffered saline (PBS) was used as a lubricant, and all experiments were performed on the pin-on-disk tribometer with reciprocating motion. The sliding speed was set to 0.5 mm/s with stroke 7.85 mm. The load of AC sample varied and its values were between 0.9 - 24.3 N, which corresponds with 0.32 - 0.96 MPa of contact pressure. All experiments were performed in the still loaded mode (without rehydration) and also in mode when the sample was unloaded always before sliding motion (rehydration). There is a significant difference between CoF with and without rehydration. The CoF value is lower with

shorter duration of experiments. The experiments with sample from highly loaded region M1 show significantly better values of CoF than samples removed from M4. The dependence between load and CoF corresponds with most previous works; the values of CoF decrease with increasing load. The contact pair of glass and AC sample is also tested by Moore A. C. et al. [10] in his study. Author tested different diameters of AC samples (6, 12 and 19 mm) and its impact on the CoF trends, and further there are experiments focused on the rehydration and its description, resulting in theoretical explanation of hydrodynamic hypothesis of tribological rehydration. The tests were carried out on the pin-on-plate tribometer, where the AC sample under a glass plate, which allows for in situ view of the contact. The authors used it for measuring of the diameter of the contact area. The contact load was set to 5 N, which corresponds with  $0.25 \pm 0.05$  MPa and  $5 \pm 0.4$  mm diameter of contact area. The experiments were performed with a sliding speed of 60 mm/s and stroke of reciprocating motion 20 mm. The results show significant decrease of CoF levels in AC samples of diameters 12 and 19 mm (see Fig. 2.1-A). The authors explain this phenomenon by the contact size ratio and size of AC sample. If the diameter of the contact area is larger than the diameter of the AC sample, friction will strongly increase (Fig. 2.1-A), and similar situation occurs with the compression rate (Fig. 2.1-B).

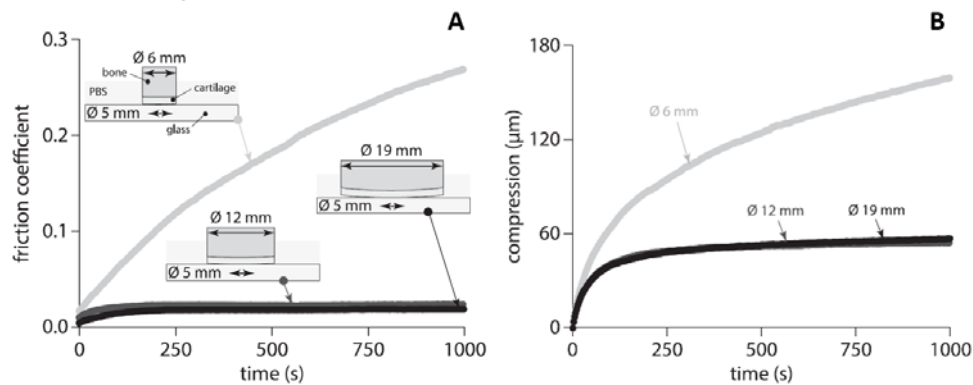


Fig. 2.1 – Friction tests – load 5 N, sliding speed 60 mm/s, stroke 20 mm, A – The impact of AC sample diameter change on CoF level; B – compression of AC samples by the same load 5 N [10]

Authors of this study also focused on the effect of rehydration due to hydrodynamic effect to friction and compression of AC sample. The experiments were carried out on sample with diameter 19 mm. The rehydration through the experiment has positive impact on the CoF value and also on the compression ratio. When the rehydration occurs, the CoF value drops to its initial value; however, the compression ratio is reduced by only about a third. The authors offer a schematic description of the rehydration due to phenomenon of hydrodynamic effect. The initial phase (no sliding speed – phase (1)) is characterized by the highest rate of fluid flowing from the AC pores to the bath, therefore the compression rate rises steeply. The fluid flowing from the AC pores is slower in the second phase (still no sliding speed – phase (2)), which causes the compression to approach an asymptote. When the sliding speed in the contact occurs, raising of the compression rate stops,

the trend of compression ratio begins to decrease, and the CoF trend falls down (phase (3) – sliding speed 60 mm/s). Authors explain this change by hydration of the AC pores by fluid due to hydrodynamic pressure, therefore the compression ratio decreases. After a certain time (phase (4) – still sliding speed 60 mm/s), the compression ratio, again, approaches an asymptote, nevertheless from the other side, and the imbibition rates balance the exudation rates. The CoF level does not change. When the sliding speed changes to lower level, the compression rates again begin to raise along with the CoF value (phase (5) – change of sliding speed to 10 mm/s). The flowing of fluid into the AC pores goes down, which causes the raise of compression and friction.

The field of biotribology of NSJ does not only include studies dealing with the friction behaviour of the AC, but there are also studies focused on defining the lubrication system prevailing in the AC contact. Studies with this focus are not very common, especially in further past, however, they are starting to appear in increasing numbers. The basis of understanding of lubricating system of the AC is described by porous structure influence, due to which the AC has unique tribological and mechanical properties. Greene G. W. et al. [11] performed a study dealing with synovial fluid (SF) flowing through the AC structure. The AC structure contains negatively charged proteoglycans, which cause proteoglycans to bind to HA, making the AC structure very highly hydrophilic (attracting water) [12]. This combination is entangled in collagen fibres on the AC surface, creating the gel-like layer on the AC surface. The diameter of pores in uncompressed state is less than 10 nm, and after compression of the AC, the diameter decreases. Size of the pores is an order of magnitude smaller than the collagen fibres, therefore the water is flowing or defunding through them [13]. When the AC is compressed, the size of the pores decreases and the flowing of water is limited. This aspect causes retention of water in the AC pores which allows for better load transfer. The pressured AC structure allows for the fibrous tissue to be held together, therefore, the mechanical properties in tension are improved [14]. The authors in [11] performed experiments with pork AC removed from knee and the AC sample was placed between two glasses plates. Fluorescently marked lubricants were used for the experiment. The AC sample was compressed by the glass and the contact was excited by laser. The fluorescence microscope was used as an observational optical device. The observation was focused on flowing of lubricant from the AC pores and the intensity of emitted light from contact was recorded. The authors also studied recovering ability (hydration) of the AC, where the amount of lubricant in dependency on time were observed. The results confirmed the hydration ability of the AC in uncompressed state, however the hydration in compressed state has also been demonstrated. Uncompressed state of the AC allows for flowing of lubricant through the AC structure in both horizontal and vertical direction. This phenomenon is allowed by two types of pores, vertical and horizontal. The flowing of lubricant through and out of structure fundamentally affects the EM through compression process. The scheme of this is given in Fig. 2.2. In the first state

(uncompressed state Fig. 2.2-A), the AC has high elasticity modulus (EM) and high load is required to open the structure to flowing. When the AC is subjected to compression, the horizontal pores begin to expand at the expense of the vertical pores, which shrink with compression. The flowing of lubricant out of the structure begins, especially from the vertical pores (Fig. 2.2-B). When larger compression occurs, the EM is low due to low lubricant volume in the AC structure. The horizontal pores are flattened and the flowing or diffusion of lubricant is difficult, therefore limited (Fig. 2.2-C). The last state of compression process is a state in which the collagen fibres are touching each other. The content of lubricant is very limited and the whole load is transferred by the solid phase of the AC structure. The load required for deformation is higher, which causes the increase of EM. The last state of compression process is shown in Fig. 2.2-D. The compression of the AC structure causes weeping of lubricant out of the AC pores, creating the lubricating film in the contact. This phenomenon is allowing the extrusion of the lubricant out of the AC structure, which works as a pump of lubricant to the AC contact. This principle is the basis of lubricating processes in the SF. It creates the basis of all models of lubricating modes and theories.

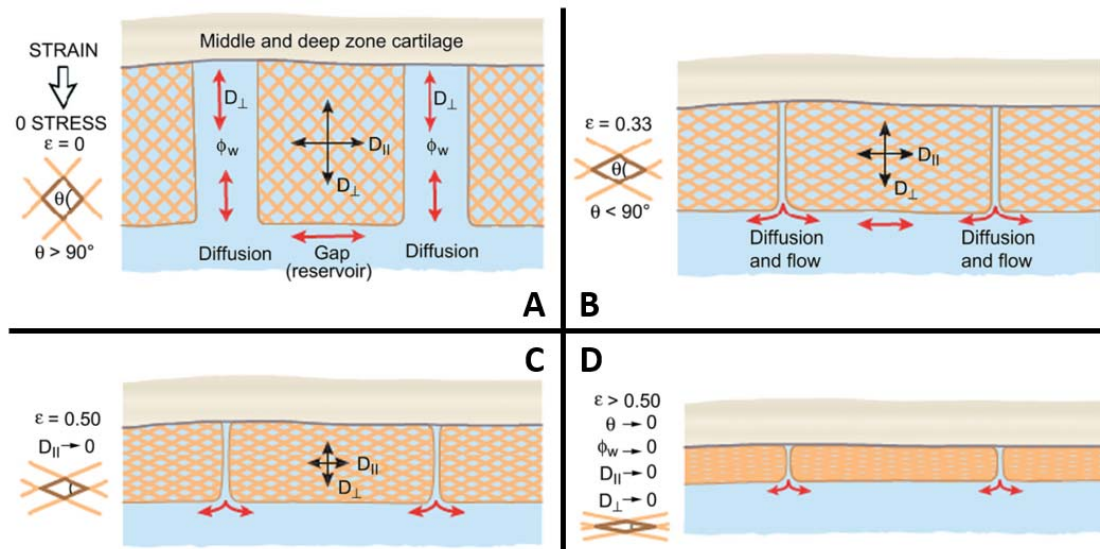


Fig. 2.2 - Compression process [11]

The Stribeck curve is an important tribological criteria, based on which the tribological properties are evaluated. The Stribeck surfaces were used in [15] by Gleghorn J. P. et al. to evaluate the tribological properties of the AC. The authors set two configurations of testing sample of AC (pivoted rod system (Fig. 2.3-A) and cylindrical rod system (Fig. 2.3-B)) and wide range of experimental conditions, from which the Stribeck surfaces were composed. The experiments were carried out with three types of lubricants, PBS, bovine synovial fluid (BFS) and unique synovial fluid (ESF). The authors constructed the Stribeck surfaces for both types of testing samples and for PBS and ESF. If the AC sample is mounted by cylindrical rod, the Stribeck surface shows a significant break between the boundary and mixed regions (Fig. 2.3-C), which the sample mounted on pivoted



rod does not report (Fig. 2.3-D). The authors justify the significant break of Stribeck surface, in case of the tests with cylindrical rod, by presence of wedge gap, which causes the hydrodynamic pressure in the AC contact. The experiments with PBS and ESF show that the ESF used as a lubricant gives several times lower values of CoF in the boundary region than PBS, nevertheless the CoF values in the hydrodynamic region are similar.

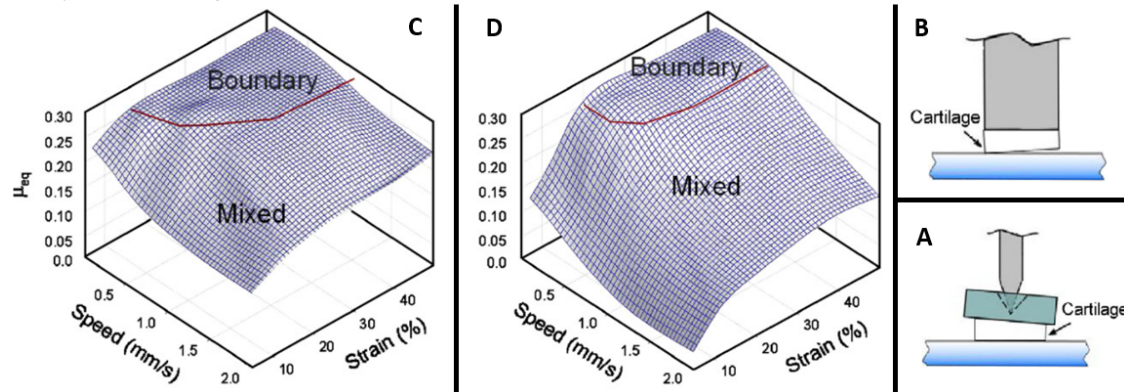


Fig. 2.3 – A - AC mounting by pivoted rod; B - AC mounting by cylindrical rod; C, D - Stribeck surfaces from mean CoF, lubricant PBS. C - pivoted rod; D - cylindrical rod [15]

In addition to the basic types of lubricating regimes that were mentioned e.g. in [16], [15], there are only few studies focused on the description of lubricating regimes, that were published so far. Until recently, there were only a few basic models of AC lubricating, weeping [17], boosted [18], biphasic [19] and boundary [20] AC lubricating regime, and only recently have these been expanded by Murakami T. et al. in [21], which adds another model - adaptive multimode lubrication mechanism (see Fig. 2.4). The adaptive multimode lubrication mechanism draws all mentioned regimes together into one group, and it says that the regime changes with operation conditions. The NSJ can respond to change of operation conditions and adapts the lubricating mechanism, while maintaining the protection of the AC. The adaptive multimode lubricating mechanism explains the difference between the Stribeck curve for hard contact (e.g. artificial joints) and AC contact. Due to the unique structural properties of the AC, the CoF stays at low levels, despite the sliding speed being very low; in this case the biphasic lubrication is active. The load is transmitted by reaction from solid phase of AC on one hand, and on the other hand the load is transmitted by reaction force from pressure of SF captured in the AC structure. When low sliding speed occurs in the AC contact and it is loaded by low force, the lubricating regime is different in each place, depending on the surface irregularities of the AC. The places that are in contact operate in boundary, hydration or gel-film lubrication; these places are the most prone to damage. The rest of the surfaces that are not in direct contact with the second cartilage, are lubricated by weep lubricant from cartilage structure. The hydrodynamic pressure begins to gain importance when the AC contact is loaded

with high sliding speed, and the adaptive multimode mechanics is suppressed, therefore the hydrodynamic lubricating regime occurs.

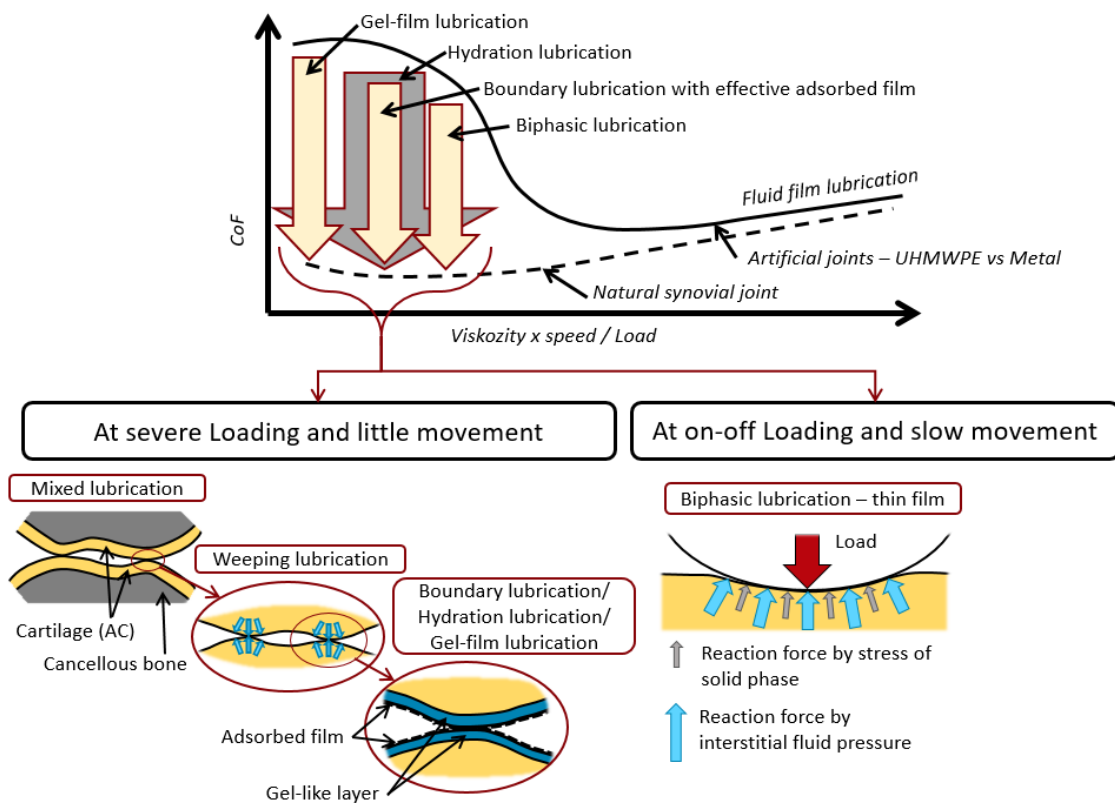


Fig. 2.4 - Adaptive multimode lubricating mechanism [21]

The principle of hydration lubrication was described by Jahb S. et al. [22]. The study was focused on modelling the NSJ by two plates of mica opposite each other. The mica plates represent the AC surfaces with similar hydrophilicity properties, which allows the specific chemical properties of lubricating film. The authors simulated the lubricating model by AFM, therefore in micro scale. Friction effects were monitored, and based on them, the theoretical model of hydration lubrication mechanism was described. Due to similar hydrophilicity of mica and AC, the bonding of lubricant components is possible. The HA creates surface layer on the mica plate due to its hydrophilicity, which creates suitable conditions for bonding of phospholipids. The phospholipids bond the HA and also bond themselves with lipid tails, which creates the phospholipidic bilayer (see left Fig. 2.5). When both mica surfaces are covered by phospholipidic bilayers, the so-called hydration shell is formed (see Fig. 2.5-B). If sliding occurs between the mica plates, the slip phase is on the borderline between both phospholipidic bilayers in the middle of hydration shell (see Fig. 2.5-B). Due to charge of phosphate core, the water in vicinity (lubricant) bonds to phosphate core. Sliding between plates causes exchange of water molecules between individual phosphate cores (Fig. 2.5-A);

therefore, the friction process takes place here (Fig. 2.5-B). High energy is necessary to break the hydration shell; therefore, it can transfer high load.

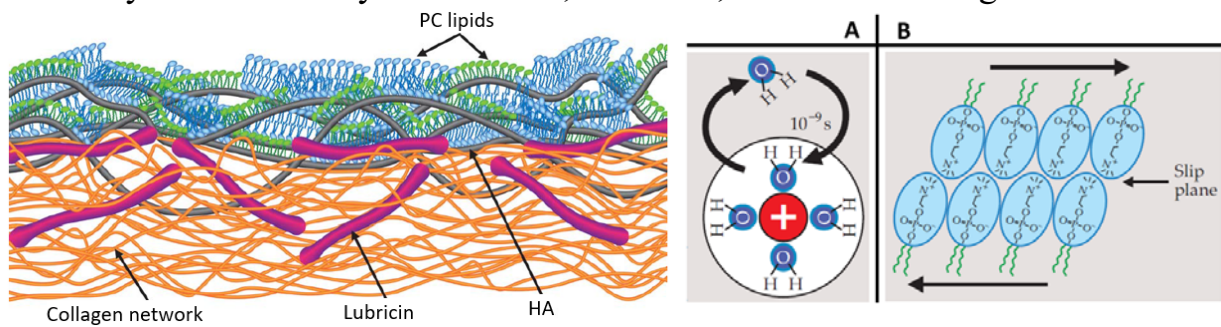


Fig. 2.5 – In the left - phospholipid bilayer on the cartilage surface; In the right - Hydration shell – the principle of hydration lubrication. A – exchange of water molecules from the vicinity and between phosphate cores; B – the hydration shell – position, where the sliding occurs [22]

The unique structure of AC is undoubtedly one of the basis properties allowing the movement of NSJ nearly without friction, however, for long-term movement, the protection of AC surface, in which the gel-like layer fulfils its role, is necessary. The significance and impact of individual lubricating mechanisms have been investigated by several authors in the past; however, the main focus was on the importance of the gel-like layer and adsorbed film. The presence of the gel-like layer was presented e.g. by Forsey R. W. et al. [23], where the reciprocating experiments between cartilage pin and plate were performed. Furthermore, the AC samples were evaluated on penetration of AC surface by HA, which creates the gel-like layer. The evaluation was allowed due to fluorescently marked HA. The results show that the HA targets defects on the AC surface and it tends to cling to chondrocytes under the AC surfaces, which is allowed only to smaller molecules of HA and the rest remains on the surface and creates the gel-like layer (Fig. 2.6-A). Therefore, the HA plays important role in damaged NSJ, where the damaged regions are protected by it (Fig. 2.6-B).

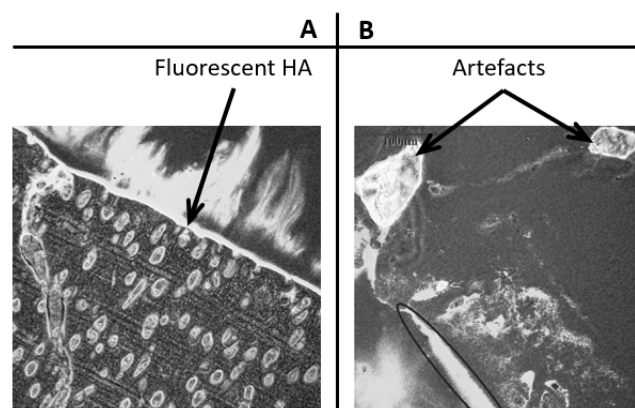


Fig. 2.6 – The bovine AC surfaces in 600x magnification; A – AC surface is coated by HA; B – HA targets to the artefacts [23]

The importance of the gel-like layer on the AC surface and its function at protecting the AC was published by Murakami T. et al. [24]. Authors carried out the experiments and based on them, the impact of the gel-like layer on the AC surface was specified. The presence and importance of the gel-like layer and adsorbed protein film on the AC surface were approached by Higaki H. et al. in their study [25]. The surfaces are covered by gel-like layer, and the protein film is adsorbed on it (see Fig. 2.7). The importance of gel-like layer in the role of a wear protector were proven, and frictional tests confirm this.

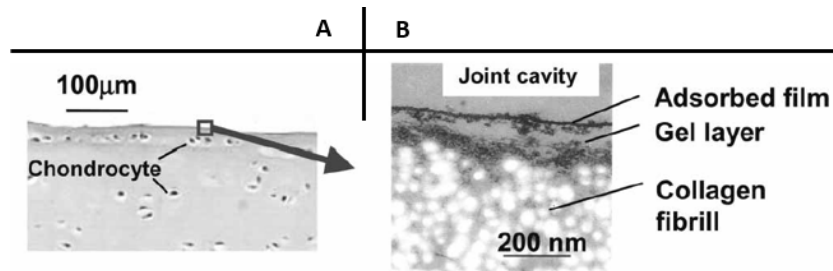


Fig. 2.7 - Surface structure; A - snap from optical microscope; B - AC transverse section [25]

Several studies investigate the AC contact using more methods simultaneously, as was mentioned earlier. However, one of the methods is always the friction measurement, which the authors combine with the other methods. For better understanding of lubrication mechanism in the AC contact, the visualization of its contact is the most useful method. The studies focused on simultaneous friction measurement and visualization are rare and the PVA hydrogel is predominantly used instead of the AC sample. Such focused research was published by Seido Y. et al. in studies [26] and [27]. Both of these studies are focused on visualization of the PVA hydrogel contact during reciprocating test, and the impact of different lubricants (especially the role of individual parts of the lubricant in film formation) was examined. The reciprocating tribometer in pin-on-plate configuration was used as an experimental device. The PVA hydrogel was used as a pin sample doing the motion, while glass was used as a plate. The fluorescence microscopy was used as a suitable optical method for visualization. The fluorescent snaps of the contact were taken always after fixed time, always before and after experiments; the visualization was not performed during the reciprocating experiment. The results show the importance of  $\gamma$ -globulin protein in formation of the lubricating film. As is evident, the lubricants containing  $\gamma$ -globulin protein report more protein clusters, nevertheless there is a strong dependence on the ratio of lubricant components. Authors monitored number of particles in the contact during the experiments, and the dependency between number of particles and lubricant composition arose (see Fig. 2.8). The clusters created by the  $\gamma$ -globulin also show higher amounts (Fig. 2.8-A) than the clusters created by albumin proteins (Fig. 2.8-B). The simple protein solutions show no significant gradual adsorption during the experiment, which is the same in both cases in which both components are marked (lubricant A, B, E, F in Fig. 2.8). When the lubricant is

more complex, such as the solution of albumin and  $\gamma$ -globulin, the number of particles is rising during experiments, nevertheless this phenomenon only applies to specific concentration of both components of the lubricant (albumin – 0.7 wt%,  $\gamma$ -globulin – 1.4 wt%), Such concentration is shown by lubricant C<sub>G</sub> and C<sub>A</sub>. in Fig. 2.8. The lubricant, with marked  $\gamma$ -globulin gives higher values of particles in the contact, therefore the increase is steeper. The lubricants that contain both components in the same ratio (D<sub>G</sub> and D<sub>A</sub>) show also increase of adsorbed particles in the contact; however, the increase stops during the experiment. Although more complex lubricants show lower number of particles, the gradual increasing of the number of particles is guaranteed. The highest number of particles in the contact is shown in simple lubricant B and F, both of which contain higher concentrations of components; consequently, a higher concentration of simple solution means a higher number of particles. The results show that the  $\gamma$ -globulin proteins adsorb in the contact first, and only then the albumin proteins adsorb on the  $\gamma$ -globulin layer.

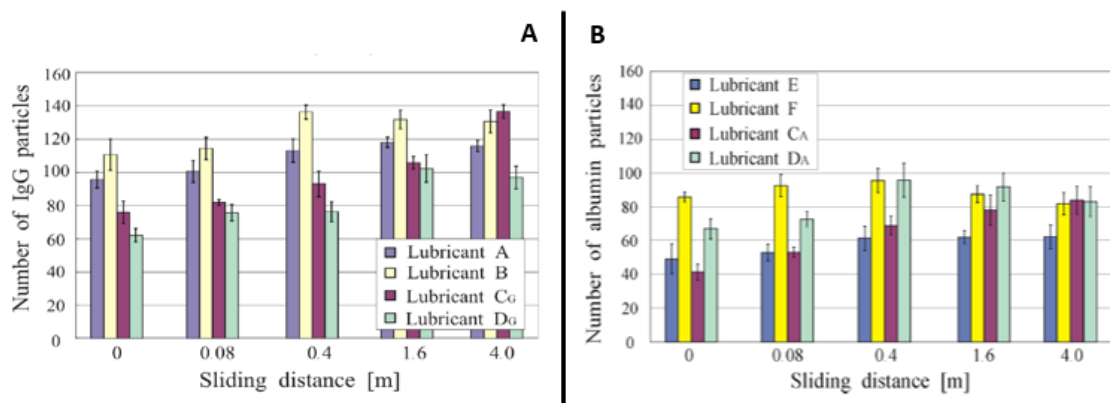


Fig. 2.8 - Number of particles during friction reciprocating test. A - marked component -  $\gamma$ -globulin solution (A, B - simple  $\gamma$ -globulin solutions - A – 0.7 wt%; B – 1.4 wt%; C<sub>G</sub> – albumin 0.7 wt% +  $\gamma$ -globulin 1.4 wt%; D<sub>G</sub> – albumin 1.4 wt% +  $\gamma$ -globulin 1.4 wt%); B – marked component – albumin (E, F - simple albumin solutions - E – 0.7 wt%; F – 1.4 wt%; C<sub>A</sub> – albumin 0.7 wt% +  $\gamma$ -globulin 1.4 wt%; D<sub>A</sub> – albumin 1.4 wt% +  $\gamma$ -globulin 1.4 wt%) [27]

A schematic model of formation of the lubricating film by the proteins components contained in the SF was published by Nakashima K. et al. [28]; however, the model is valid for hydrogel contacts. The authors performed reciprocating test and the additional analysis was performed after the test. The analysis was focused on composition of the adsorbed film from PVA hydrogel vs glass reciprocating test. The glass sample was observed after the experiments, and the adsorbed film was gradually removed. After each removing of the adsorbed film, the analysis of the film was performed using fluorescence microscope. Authors divided removal of the adsorbed film into three steps – the surface zone, the middle zone and the deep zone. Several configuration of lubricant were used for testing; each one combined albumin and  $\gamma$ -globulin protein in different ratio. The snaps from fluorescence microscope were taken sequentially, and both snaps were put together in the end. The best results were shown by the lubricant containing both proteins (albumin and  $\gamma$ -globulin); however, the specific ratio is

required (0.7 wt% of albumin and 1.4 wt% of  $\gamma$ -globulin). The snap of this experiment is shown in Fig. 2.9-A. The lubricant with reversed composition (1.4 wt% of albumin and 0.7 wt% of  $\gamma$ -globulin) does not show such good results (see Fig. 2.9-B) compared to Fig. 2.9-A. Based on the results of gradual analysis of the glass plate, a lubricating formation model was compiled. The best variation is the already mentioned lubricant shown in Fig. 2.9. The lubricant being only a simple protein solution reduces the wear, but only a little. The last variation shows the model of lubricant with too much protein content, which causes increase in wear.

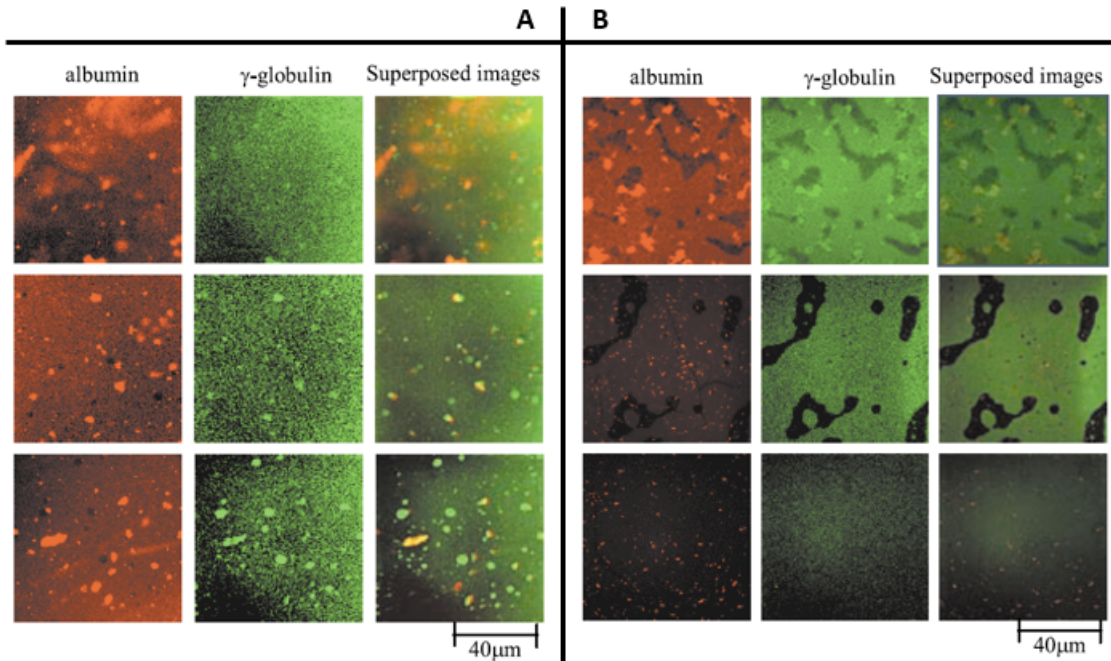


Fig. 2.9 – Fluorescence snaps of glass plate after the reciprocating experiment. A – lubricant composition - albumin 0.7 wt%,  $\gamma$ -globulin 1.4 wt%; B - lubricant composition - albumin 1.4 wt%,  $\gamma$ -globulin 0.7 wt% [28]

### 3 ANALYSIS AND CONCLUSION OF LITERATURE REVIEW

From the literature review, it is obvious that biotribology of NSJ is very important and currently developing field, trying to describe the lubrication processes prevailing in the NSJ. The review shows that the lubricating processes in the NSJ are not fully described, nor fully understood yet.

The NSJ is a unique tribological object allowing for movement with very low friction [9]. The basis of friction properties of NSJ is the AC in combination with SF. The AC is a compliant porous material allowing for fluid retention, and the EM is very low [9], [11]. Studies focused on the tests of AC confirmed that the SF is a unique lubricant, most frequently reporting the lowest CoF [7]. The AC shows a dependency between CoF and load, the CoF is decreasing with increasing load [7], [8]. The CoF is also affected by the region from which the samples are removed. The samples removed from a more loaded region show better frictional properties than the samples removed from the regions outside the loaded region; this phenomenon is linked with mechanical properties of the samples [9], [8]. Furthermore, rehydration of AC in between friction tests positively affected the CoF trend. The CoF trend is restarted to the initial value [21], [8], [10]. The positive impact of hydrodynamic pressure in the AC contact is described by [16], [15].

The efficiency of the AC lubrication is expressed by CoF; however, the explanation why the CoF is uniquely low is important for full understanding of the NSJ lubrication. The basis of NSJ lubrication are the structural properties of AC, which allow flowing of the lubricant into, away from, and through the structure of the AC [11], [16]. This phenomenon allows for the hydration of cartilage, and the weeping of the lubricant from the AC structure is the basis of the lubricating theories [21], [11], [10], [17], [18]. The flowing of the lubricant through the porous structure is dependent on the lubricant composition and the amount of lubricant contained in the structure influences the EM of the AC, which varies with compression rate [11]. The size of molecules of individual components in relation to the size of pores is a crucial criterion for penetrating the porous structure. The components with larger size of molecules create the layer on the AC surface [21], [22], [23], [25], [28]. The surface layer is the basis for low friction, and it is very important for AC protection [23], [25]. The layer, which is created on the AC surface is composed of two basic components – gel-like HA layer and adsorbed protein film [21], [22], [23], [25], [28]. The gel-like layer bonds the chondrocytes in the AC structure located directly on the AC surface [23], [24], [25]. This layer is responsible for protection of the AC covering the defects on the AC surface [23], [25]. The adsorbed protein film is formed on the gel-like layer and is an order of magnitude thinner [22], [25]. The adsorbed film causes the specific function of AC lubrication, such as the hydration lubrication [22]. The adsorption rate depends on the lubricant composition, especially on the ratio between the protein components in the

lubricant; however the studies were focused only on testing of PVA hydrogel [26], [27], [28]. The main role in the formation of the lubricating film in the PVA hydrogel contact is played by the protein  $\gamma$ -globulin, but also by the right composition and the ratio between the components to adhere to [27], [28].

Based on the literature review, the only suitable optical method for simultaneous visualization of the AC contact lubricated by SF is fluorescence microscopy [23], [25], [26], [27], [28]. This method allows for the observation of individual components marked by fluorescence dye [26], [27], [28]. The observation of individual components allows for the description of lubricating film formation in the AC contact. The visualization limitation is the necessity of using a transparent material as one part of the testing pair; in this case, it is mostly glass, which, of course, affects the contact area e.g. from the point of view of the EM or contact pressure [10], [26], [27], [28]. Such focused studies are very rare; however, the authors used PVA hydrogel instead of AC [26], [27], [28], or simultaneous visualization is not performed [10]. The studies dealing with the evaluation of the adsorbed film exist but the evaluation is performed after the experiments [23], [25].

The literature review shows that the research dealing with tribological behaviour is very widespread, and its tradition dates back several decades. There are many studies dealing with friction behaviour of AC, especially the studies that have been published further in the past. Topics of these studies are diverse and it is obvious that the frictional behaviour of NSJ is well described. On the other hand, there are works focused on the lubricating issues of the NSJ. These works deal with formation of the lubricating film in the AC contact. There are many theories trying to describe and explain the mechanism of AC lubricating; however, only a few of them have an experimental background. There are also studies that perform tests to describe the lubricating film formation in the AC. These studies use the method of simultaneous visualization of the contact and friction measurements; however, they use PVA hydrogel samples instead of AC samples. There is no study, which would use the simultaneous visualization and friction measurements in the AC contact to describe the lubricating film formation. It follows that the lubricating issues are not fully understood, and there is no study that would provide a full description of lubricating film formation in the AC contact.



## 4 AIM OF THESIS

The aim of this PhD thesis is to describe the effect of individual components of synovial fluid on lubricating film formation in the model of synovial joint. The thesis is focused on the experimental analysis of friction coefficient and observation of adsorbed lubricating film with the use of the principle of fluorescence microscopy. To achieve the main goal of this thesis, the solution to the following sub-aims is necessary:

- Development and design of the experimental device.
- Development of the methodology for removing and storing of the articular cartilage samples.
- Design of the methodology of experiments.
- Design of data processing and evaluating.
- Series of experiments focused on the analysis of the influence of individual components of synovial fluid.
- Data analysis.
- Discussion and publication of obtained results.

### 4.1 Scientific questions

- What is the influence of the individual components contained in the model synovial fluid on the lubricating film formation in the model of synovial joint?
- How is the friction coefficient affected by the number of dominant protein particles in the model of synovial joint?

### 4.2 Hypotheses

- A simple protein solution does not create a stable lubricating film with high friction coefficient. A combination of simple proteins causes the proteins to bind to each other. Forming of the lubricating film is mostly affected by hyaluronic acid and phospholipids; these components contribute to the stability of lubricating film and increase its thickness.
- It is expected that a higher particle count of dominant proteins component adsorbed in the contact causes a higher friction coefficient whereas the thickness and area of lubricating film increases.

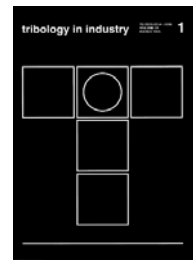
### 4.3 Thesis layout

The PhD thesis is composed of one paper published in peer-reviewed journals and two papers published in journals with impact factor. The first article is focused on development and design of the experimental device. The design of reciprocating tribometer that allows for simultaneous visualization and friction measurement is described. The experimental device containing a fluorescence microscopy is introduced. Initial experiments involving simultaneous friction measurements and AC contact visualization are performed. The second article is focused on the methodology of the experiments. Evaluation of the experimental data is described. Furthermore, processing of the experimental data from the fluorescence visualization is described, including the software for evaluation. The principle of the snap processing is described in detail, and calibration of the fluorescence method is examined. The last article is focused on the application of designed experimental approach. The experimental set focused on determining the influence of the albumin protein on lubricating film formation was performed. The analysis of the influence of individual components and their role in lubricating film formation is described. This article is a combination of two previous ones, where the main aim of this dissertation thesis is answered

- [29] ČÍPEK, P.; REBENDA, D.; NEČAS, D.; VRBKA, M.; KŘUPKA, I.; HARTL, M. Visualization of Lubrication Film in Model of Synovial Joint. *Tribology in Industry*, 2019, 41, 387-393.

*Author's contribution: 70%*

**CiteScore = 1.09**



- [30] ČÍPEK, P.; VRBKA, M.; REBENDA, D.; NEČAS, D.; KŘUPKA, I. Biotribology of Synovial Cartilage: A New Method for Visualization of Lubricating Film and Simultaneous Measurement of the Friction Coefficient. *Materials*, 2020, 13, 1-20.

*Author's contribution: 50%*

**Journal impact factor = 3.057, Quartile Q2, CiteScore = 3.26**



- [31] ČÍPEK, P.; VRBKA, M.; REBENDA, D.; NEČAS, D.; KŘUPKA, I. Biotribology of synovial cartilage: Role of albumin in adsorbed film formation. *Engineering Science and Technology, an International Journal*, 2022, 34: 101090.

*Author's contribution: 50%*

**Journal impact factor = 4.36, Quartile Q2, CiteScore = 9.00**



## 5 MATERIALS AND METHODS

None of the commercial tribometer allowed for simultaneous visualization of the contact area and friction measurements. Furthermore, the reciprocating motion and low loading are necessary to accomplish the aims defined in the previous chapter. In order to comply with all of these requirements, the self-designed tribometer was developed. The conception of the tribometer was inspired by the previous studies where the visualization of the contact area was performed. The experimental device used in [10] fulfils the requirements for simultaneous visualization and frictional measurements, and the location of the contact area corresponds with the optical device used by our department [32]. The requirements for experimental conditions were set based on the previous studies and real conditions prevailing in the human natural joints [33], [10].

The scheme of the self-designed reciprocating tribometer is shown in Fig. 5.1-A. The AC sample is located under a glass plate, and it is static. This arrangement allows for continuous observation of the AC contact by fluorescence microscope, and the contact area is recorded by a high-speed camera. The contact is flooded with the lubricant (model synovial fluid in this case) and the bath is heated to the human body temperature. The second part of the contact pair is the glass plate, which is the movable part producing the reciprocating motion. The AC sample is mounted to a lever, which is fixed by a shaft and bearings. The load on the contact is applied through the AC sample by lifting of the lever by the linear stepper motor placed under the lever. The basis of the tribometer is a rigid frame, allowing for rigid mounting of the movable parts, and movement without clearance. The movable glass plate is mounted on the carriage, which is fitted by a ball sleeve. The carriage motion is allowed due to its mounting on the guide bars and the carriage is reciprocally propelled using a ball screw and stepper motor. The sealing between the glass plate and the heated bath prevents leaking of tested lubricant from the bath. The device is equipped with two load cells to examine the CoF during the experiment. One sensor detects the load force (normal) and the second one the friction effects. The whole device is placed under the fluorescence microscope allowing the contact observation during the experiments (see Fig. 5.1). The Arduino MEGA 2560 microcomputer (Atmel Corporation, San Jose, USA) is responsible for controlling of the movable parts of the tribometer; detection of the effects of the forces is allowed by the measuring card NI USB 6001 (National Instruments, Austin, Texas, USA). The effects of the forces are recorded by computer and LabVIEW software (National Instruments, Austin, Texas, USA) using a measuring card. The measuring and controlling equipment are located in the control box connected with the tribometer by cables. The experimental conditions (e.g., sliding velocity, stroke, load during the experiment, etc.) can be modified on the control box using control buttons and display.

## 5.1 Fluorescence microscopy – visualization method

The optical method based on fluorescence principle was used for the observation of the AC contact. Fluorescence is the light emission of the substance. The fluorescence emission occurs when the substance is excited by light or other electromagnetic radiation; the excited substance begins to emit light. The fluorescence phenomenon can be divided into three basic phases excitation, excited-state lifetime and fluorescence emission.

A detailed description of fluorescence microscopy is provided in [34]. The scheme and the experimental apparatus in the laboratory are shown in Fig. 5.1. The light source is represented by a mercury lamp emitting white light. The Fluorescein Isothiocyanate (FITC) and Tetramethylrhodamine (TRITC) filters were used for the purposes of this thesis. The filters allow for the change in the wavelength of excited and emitted light; FITC (excitation on 490 nm, emission on 525 nm) and TRITC (excitation on 557 nm, emission on 576 nm). The axial resolution of the FITC filter is approximately 290  $\mu\text{m}$ , and 320  $\mu\text{m}$  for the TRITC filter. The filter is mounted to the carousel located above the lens. Due to the large size of the compliant contact of AC, the double magnification lens was used for observation. The depth of field of the apparatus is approximately 200  $\mu\text{m}$ , which was sufficient with respect to the sliding speed and the estimated film thickness. The image focusing is performed by the field diaphragm and a slight refocusing by the z-feed of the optical system. The observation of the AC contact was performed through a glass plate made from optical glass B270; therefore, the optical properties of the glass did not affect neither fluorescence excitation, nor emission. The same apparatus was used for observation of the artificial joint contact represented by glass acetabulum and stainless steel hip joint. A description of the optical system and its use are published in [32].

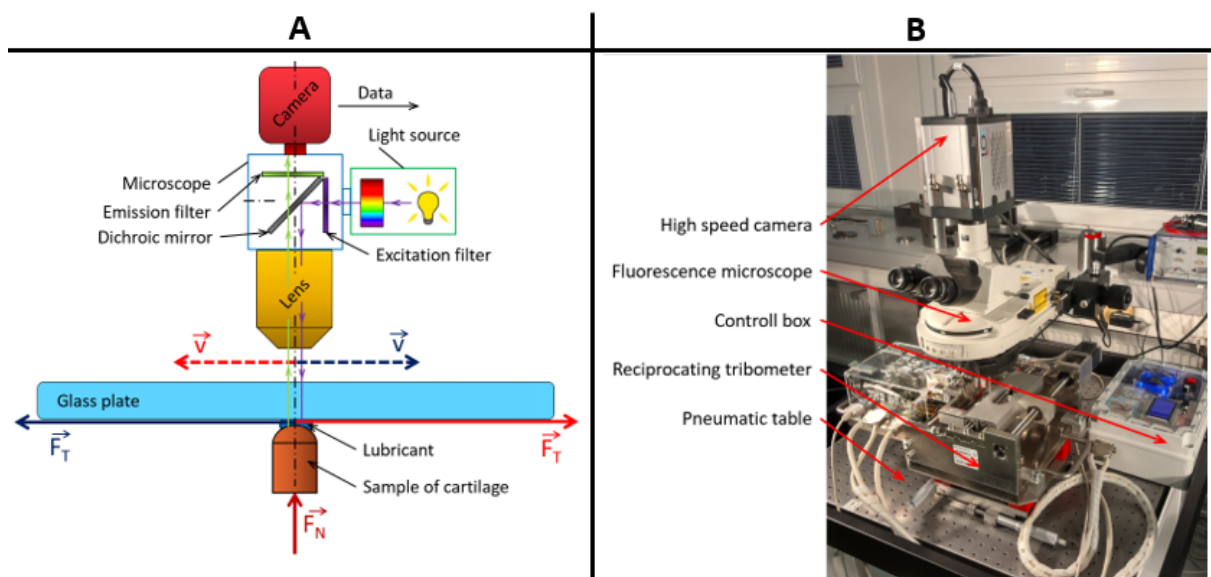


Fig. 5.1 - Fluorescence microscopy. A - Scheme of fluorescence apparatus conception; B - Experimental apparatus in laboratory

## 5.2 Specimens and conditions

### 5.2.1 AC specimens

The pin samples removed from the femoral hip head of mature pigs were used. The samples were removed as soon as possible after the slaughter of the animal from the canopy of the femoral head, and the emphasis was placed on the same location of the sampling region through all sampling femoral heads. The emphasis was also placed on preserving the undamaged surface of the sampling region. This procedure ensures that the removed samples had as similar properties as possible because the mechanical and tribological properties strongly depend on the location of the sampling region [9], [8]. The ejector and hollow drill bit were used for sample removal. At the beginning of this thesis, the hollow drill bit was used to remove the samples [29], [30] but these samples had frayed edges. To avoid this, the ejector was preferred [31]. The diameters of the samples were 5.7 and 9.7 mm. The deviation between the AC samples with different diameters was published by Moore A. C. et al. [10], where the analysis of the CoF influence on the diameter of the sample was described. The basis of the contact visualization is that the contact area has to be of a lesser diameter than the diameter of the sample itself. For the experimental tasks focused on visualization, the samples with 9.7 mm diameter were used. The removed samples were stored in PBS, deeply frozen (-20 °C) immediately after sampling, and the testing samples were defrosted immediately before the experimental set. This sampling procedure was used in [35], and verified in [36]. The second sample of the contact pair was the glass plate, which fulfils the important premise of transparency, in order to ensure an insight into the contact area. The glass plate is 154 mm long, 43 mm wide, and 4 mm thick.

### 5.2.2 Lubricants

The PBS was used as a lubricant for the verification phase of this thesis (verification of the sampling process, verification and calibration of the reciprocating tribometer). Furthermore, the model synovial fluids were used for the experimental sets, where the simultaneous visualization and friction measurements were performed. The lubricants are shown in Tab. 5-1. The basis of visualization is the labelling of observed components; in this case, it was bovine serum albumin or  $\gamma$ -globulin. The albumin (Sigma-Aldrich, A7030) was labelled by Rhodamine-B-isothiocyanate (283924, Sigma-Aldrich). In the second case,  $\gamma$ -globulin from bovine blood (Sigma-Aldrich, G5009) was labelled by Fluorescein-isothiocyanate (F7250, Sigma-Aldrich). The other components containing the model SF are HA with molecular weight of 1000 kDa and phospholipids. The experimental lubricant was prepared by mixing of all the components with PBS. The prepared experimental lubricants were wrapped in the aluminium foil to prevent degradation of the labelled components by light. The lubricant samples were stored in frozen state at -20°C. Defrosting was performed immediately before the experiment. Lubricants 1 – 4 were used in the last study attached to this work [31] for

clarification of the albumin impact on the lubrication film formation in the NSJ. Lubricants 1, 5 and 3 were used in the study [29] to examine the device functionality; the study [30] used lubricants 1, 3 and 6.

Tab. 5-1 - Lubricant composition

Lubricant label	Composition, concentration (mg/ml)				Labelled component
	Albumin	Y-globulin	HA	Phospholipids	
Lubricant 1	20	-	-	-	Albumin
Lubricant 2	20	3.6	-	-	Albumin
Lubricant 3	20	3.6	2.5	-	Albumin
Lubricant 4	20	3.6	2.5	0.15	Albumin
Lubricant 5	-	3.6	-	-	γ-globulin
Lubricant 6	20	3.6	2.5	-	γ-globulin

### 5.2.3 Experimental conditions

All experiments were performed under the conditions which correspond with the real conditions in the NSJ; they were inspired by previous studies [37], [33], [38]. Contact pressure of 0.8 MPa was used for all experiments, which corresponds with 10 N of load. The value of contact pressure was determined by the Hertz theory and corresponds with the contact pressure prevailing in the hip joint [33]; however, the value is strongly dependent on the EA of removed sample, which varies through all specimens [9], [8]. All experiments in this thesis were performed using the same load (10 N), sliding velocity (10 mm/s), and stroke (20 mm) of reciprocating motion. Variations in the duration of experiments occur. Longer duration of experiment was used for the second study attached to this thesis to verify the newly developed method of visualization of the AC contact [30]. Sliding velocity was also determined in correlation with the real conditions prevailing in the NSJ during human movement. A set sliding velocity of 10 mm/s corresponds with slow human walk. The constant velocity during every stroke is possible due to the movement system based on the stepper motor and a ball screw. The constant part of the velocity trend is approx. 97% of every cycle. The temperature of the human body was maintained during all experiments performed with the AC.

### 5.3 Methodology and experimental design

A strictly-defined procedure before, during, and after each experiment was defined and followed. The procedure allows for comparability of experiments and helps to achieve a better repeatability. Before each experiment, the sample was hydrated in PBS to avoid drying out. Due to differences between the AC samples, the run-in cycle of each tested sample was used. This cycle is composed from 20 reciprocating cycles at load of 10 N, and after that the AC sample is unloaded in order to rehydrate. This cycle allows weeping of the original SF, which was

contained in the structure of the AC before the experiment. The SF is retained in the structure and comes from the NSJ of slaughtered animal. The composition of this SF may be different; therefore, it is necessary to remove it. The run-in cycle is also used when one AC sample is tested repeatedly, for same reasons mentioned before; the lubricant contained in the AC structure needs to be removed not to affect the experiments. One AC sample is repeatedly tested to achieve comparable results from several experiments. Before each experiment, the heated bath was cleared by protein removal solution (SDS) to achieve a non-affected lubrication bath. The experimental device is covered with a dark tarpaulin to prevent access of light from the outside; therefore, the fluoresce excitation and emission are not affected during the experiments. Repeated experiments, performed in the third study attached to this thesis [31], were carried out with a rehydration cycle between experiments. The aim of these experiments was to determine the impact of rehydration together with verification of repeatability. Nine experiments were performed in each set, which is defined by designed arrangement of the experiments. The experimental set was divided into three repeated experiments. The rehydration lasting 2 minutes was carried out after each experimental task. The rehydration causes restarting of CoF to the initial value, which allows for the use of this phenomenon to perform each experimental task as a unique one. This arrangement allows for the comparison between the experiments in terms of repeatability, while maintaining the comparability between them (experiments with one sample).

The outputs of each experiment are the records of forces representing their effects, and recorded snaps represent visualization. One of the aims of this thesis was to design the methodology of experimental data evaluation. The evaluation scheme is given in Fig. 5.2. Each experimental output has to be post-processed in two ways, the friction data processing and the visualization data processing. Raw data from the forces effects are time, normal load and friction forces. This data is saved by computer with sampling frequency of 50 Hz. The friction force is shifted due to preloading of the friction sensor. This allows measuring of the friction forces in both directions during reciprocating motion. The offset of friction force trend is deducted using deduction of mean value (Fig. 5.2-A). It causes shifting of the friction force trend around the zero axis. Furthermore, the CoF is calculated by dividing the friction and load force. Due to the reciprocating motion, CoF has an alternating trend around the zero axis. An absolute value is created from all CoF values. The reciprocating motion causes that the CoF takes the zero value when the carriage is in the extreme positions. These values are deleted based on the difference between two adjacent values; when the difference is greater than the decision value, the CoF value is deleted Fig. 5.2-B). The decision value was set based on the experience from the tuning phase of the evaluation process. Recordings of trends of the effects of forces start immediately before and after the experiment. The overlap has to be cropped. Based on the initial movement of the sample during the experiment, a peak of friction force appears in its trend, which allows us to determine the moment of the beginning of the experiment.

The CoF trend is the first criterion that is evaluated from the effects of forces (Fig. 5.2-C). The second one is the percentage difference between the beginning and the end, which is determined from the average of the last 1000 and first 1000 values of CoF.

The second parallel input into the evaluation procedure is a visualization record. The high-speed camera saves the record with the sampling frequency of 8 snaps per second, which can be modified based on the needs of the user and the capacity of hardware. Recorded snaps are saved with resolution of 2560 x 2140 pixels, which creates the pixel size of 3.75 micrometres with double magnification lens (Fig. 5.2-D). The specially designed software for snap evaluation was designed to remove the background and highlight lighter points (labelled proteins). The background is caused by optical noise and the lubricant contained in the porous structure of AC (Fig. 5.2-E). A description of the evaluation software principle is given in the paragraph bellow, and in the third study it is attached to this thesis [30]. The evaluation software calculates the particle count and their average size, which are values important for the forthcoming evaluation. The evaluation software processes every snap on record, which allows for determination of the particle count trend and the trend of average size of the particles (Fig. 5.2-F). Similar to evaluation of the effect of the forces, the values are saved immediately before the experiment, and the saving stops when the experiment ends. The beginning is detected due to the initial movement of particles on the snap. Furthermore, the trends, which are the outputs of the snap evaluation, are processed, and the percentage deviations between the beginning and the end are calculated (Fig. 5.2-G). The evaluation of the influence of SF composition is possible due to determination of deviations and trends, which were evaluated using both evaluation methods (effects of forces and visualization).

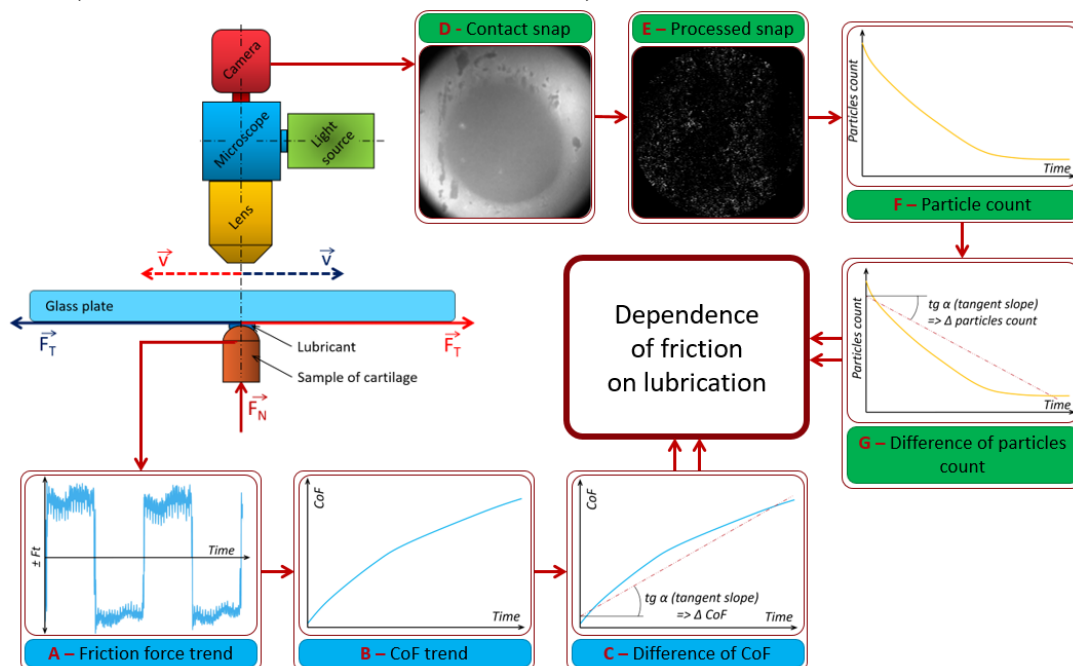


Fig. 5.2 - Evaluation scheme. A - Friction force trend; B - CoF trend; C - Difference of CoF; D - Contact snap; E - Processed snap; F - Particle count; G - Difference of particle count



The processing of snaps was based on the unique design of the software (Fig. 5.3) using the segmentation principle of image processing. Segmentation is the process of transforming the individual parts of the snap into meaningful regions or objects [39]. This software removed the background and highlighted the labelled proteins from snaps in several steps. The whole procedure of snap processing is shown in the diagram in Fig. 5.3. First, the contact area was defined by a circle (Fig. 5.3-B and Fig. 5.3-C), and the surrounding area was suppressed, i.e., the surrounding area did not enter the future processing. The contact area was defined based on visual observation; the contact area was clearly visible in each snap. In the second step, dual operations, erosion and dilation, were carried out (this combination is called morphological opening, Fig. 5.3-D); therefore, at first, the structuring element (SE) was searched for in the examined area, and if SE was detected, the pixel was added into the center of SE (i.e., the examined area was reduced by the SE radius). After that, the overlap of SE in the examined area was determined. If SE, at least partially, overlapped with the examined area, the center of the resulting area was added (i.e., the examined area was magnified by the SE radius) [39]. The opened snap was subtracted from the original snap (Fig. 5.3-D and Fig. 5.3-E). Finally, thresholding was carried out (see Fig. 5.3-F and Fig. 5.3-G); according to the threshold value, all points that were below the threshold were suppressed. This principle was used in [40]. The author used the morphological opening for processing of microscope snaps of metallic alloy to highlight some parts of the snap and remove the background.

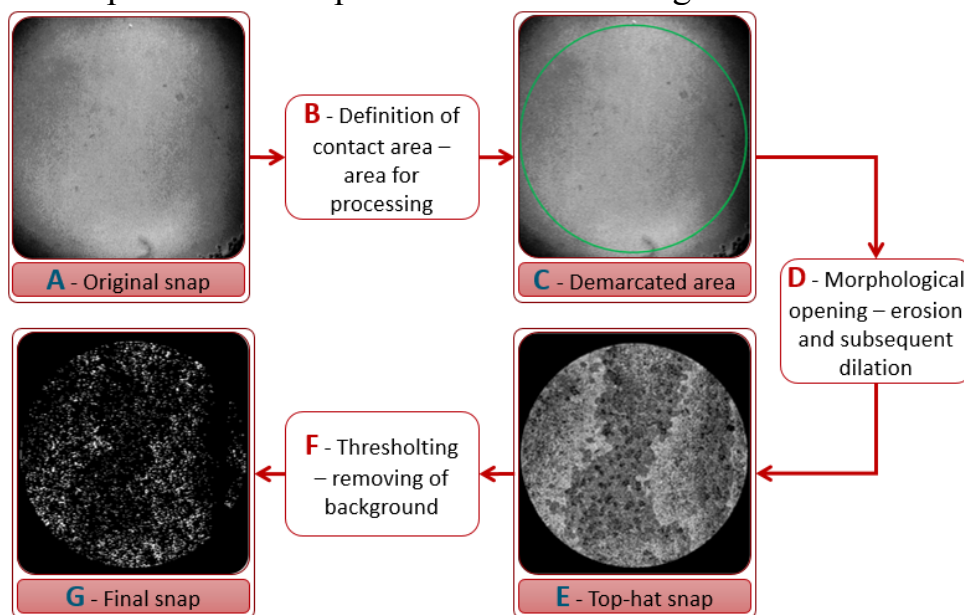


Fig. 5.3 - Snap procedure. A - Original Snap; B - Definition of contact area-area for processing; C - Demarcated area; D - Morphological opening-erosion and subsequent dilation; E - Tophat snap; F - Thresholding-removing of background; G - Final snap

## 6 RESULTS AND DISCUSSION

The verification of the AC contact using a spectrometer was carried out. Labelled proteins, used for mixing of the model SF, were tested using a spectral analysis. The combination of labelled albumin and  $\gamma$ -globulin in one solution without AC sample, the AC sample itself without lubricant and the AC sample with lubricant were tested. The FITC and TRITC filters were used for testing, and the emission was monitored. The results are published in the second study attached to this thesis [30]. The analysis shows that the individually labelled components contained in lubricants do not affect each other. Each labelled component produces light emission only in wavelength of assigned filter, and no emission was detected under other filters. The results confirm that the AC tissue emitted no light when the sample was excited by assigned filters. The conclusion from the spectral analysis is that no influence due to unwanted emission occurs. The visualization of processing procedure, including the specially designed evaluation software of snap processing, was also presented in the second study attached to this thesis [30]. This special software removes the background of snaps and highlights labelled particles (album or  $\gamma$ -globulin in this case). The essence of this software is given in chapter 5.3. The calibration of evaluation software is the basis of correct processing of snaps acquired from visualization records. The first step is to define the contact area, which is performed by definition of diameter and center of the contact area. The basic premise of the process of calibration is that the fluorescence intensity of the snap is higher when the contact contains more particles; therefore, the quantity of mean fluorescence intensity is the reference value for software calibration. This quantity is evaluated for each recorded snap, which gives us the trend of fluorescence intensity. The tangent slope for intensity trend is calculated, which represents a deviation in lubricating film between the beginning and end of the experiment. A wide range of input parameters for the evaluation software is determined (TopHat and Treshold) and every recorded snap is processed. The tangent slope for each output is evaluated. Acquired tangent slopes are compared with the fluorescence intensity outputs; the setting that shows the largest similarity to the tangent slope is determined to be correct. The correct setting is valid only for the experiments in one set, using the same lubricant (the same labelled component). If a different lubricant is used, a new calibration has to be carried out. The sensitivity analysis of the evaluation software was published in the third study attached to this thesis [31]. The analysis shows the dependency of the software input parameters in correlation with fluorescence microscopy. A wide range of input parameters is given, and the correct input parameters are located approx. in the middle of the presented range. Certain parts of the input parameters (low values of Threshold) show a linear dependency. The linearity is valid also for input parameters which are close to the setting used for snap processing. Consequently, the error caused by using another setting from the linear region is linear, i.e.,

no deviation occurs when the same setting is used for the whole set of experiments, because the results are only mutually compared.

## 6.1 Lubricating film formation in the model of synovial joint

The evaluation of lubricating film formation is based on simultaneous visualization and friction measurements, which allow for more comprehensive view of the lubricating mechanism prevailing in the NSJ. This unique approach allows for the connection between the frictional behaviour and contact observation. The particle count and their average size are used as evaluation criteria of the new approach, and the connection with CoF was established. The experiments were focused on the influence of the individual components of model SF, which is possible due to individually labelled components. The tested lubricants (model SF) were mixed from simple to more complex solutions. The evaluation was performed using a combination of the effects of the individual components in differently composed solutions, and their impact to the frictional behaviour of AC contact. Consequently, it is possible to evaluate the quantity and quality of the lubricating film. This new evaluation approach was published in the second study attached to this thesis [30], and the initial results were given. A loading process of the AC contact was observed and evaluated by the new evaluation approach, and the results show a strong decrease of particle count trend during the loading process. The following particle count trend reports only a slight decrease. The dependency between the particle count and the average size of protein particles (clusters) was found, which shows the relationship between both quantities; as the particle count strongly decreases, the average size of clusters shows a steep increase. When the contact of the AC sample with glass plate occurs, the snaps of the contact area show an outflow of particles from the contact, and the size of clusters strongly increases. This phenomenon points to a better ability of the proteins clustering when a high contact pressure (load) occurs. A very similar phenomenon was detected in studies [17], [41], where the escape of lubricant was also observed; nevertheless, this phenomenon was described only theoretically, without the experimental background. A new evaluation approach introduced in [30] was used for the experimental set focused on albumin impact on lubricating film formation, which was published in [31]. This study represents the culmination of this thesis, where the developed reciprocating tribometer [29] and evaluation methodology [30] are used for the experimental analysis in order to describe the lubricating film formation. The experimental set with a gradually composed lubricant was performed (see chapter 5.2.2). In order to evaluate the influence of the individual lubricant components, the lubricants ranging from a simple to complex protein composition were used. The simultaneous visualization and friction measurements were performed, and the outputs were processed using the introduced methodology. The best frictional behaviour was given by the lubricant with the following composition: albumin +  $\gamma$ -globulin + HA; conversely, a simple albumin solution shows the worst frictional properties. The lubricant represented by a

mixture of proteins (albumin +  $\gamma$ -globulin) shows a slight reduction of CoF. A complex model of synovial fluid (albumin +  $\gamma$ -globulin + HA + phospholipids) gives lower CoF values than protein solutions; nevertheless, the CoF values are higher than the values in the lubricant represented by a mixture of proteins and HA. A similar impact of  $\gamma$ -globulin proteins on the frictional behaviour was found in [21], [24], where the addition of  $\gamma$ -globulin proteins causes a slight reduction of CoF; furthermore, the same impact of HA was observed in these studies. The criterion for evaluation of lubricant quantity was determined in the second study attached to this thesis [30]. This criterion compiles a dependency between lubrication and friction, which is expressed by a graph where the x-axis represents *Arithmetic mean of CoF x deviation of CoF*, and the y-axis represents *Protein lubrication film area*. The x-axis expresses the frictional impact, because the use of only the arithmetic mean from the measurements can be confusing; therefore, the deviation impact was implemented. The same method was used in relation to the axis y. The resulting graph gives an overview of quality and quantity of lubricating film created in the model of the NSJ. All measurements were plotted in this graph, where four areas are drawn. Each of them represents one composition of the lubricant. The size of the areas corresponds with standard deviations of measurements and represents the stability and robustness of created lubricating film. The simple albumin solution shows the greatest area size. The particle count trend of this solution declines but the trend of the average size of clusters rises; therefore, the area of lubricating film created by albumin proteins slightly expands. A count of the albumin clusters in the contact depends on the amount of albumin particles around the contact area prior to the loading process - these particles are then trapped in the contact. The greatest area size in the resulting graph points to the lowest stability of simple protein solution; however, the adsorbed film on the AC surface is created. The albumin proteins adsorb on hydrophilic surfaces, which was shown in [42]. Consequently, the structural polarity of AC causes the attraction and adsorption of water solutions [43]; therefore, the AC surface is suitable for albumin protein adsorption. The lubricant flows through the porous structure but flowing is dependent on the size of the particles, as mentioned in [11], [44]. Due to the pressure gradient, the albumin proteins create clusters larger in size, which is the reason why the CoF shows higher values. The second tested lubricant (albumin +  $\gamma$ -globulin solution) shows lower values of CoF than the previous one, and the particle count also declines during the experiment but the decline is steeper. The adsorbed protein clusters show a lower average size, which corresponds with a lower area of lubricating film in the resulting graph. The  $\gamma$ -globulin proteins are much bigger than the albumin proteins, and due to its structural properties, the  $\gamma$ -globulin binds the albumin, which corresponds with [45]. The  $\gamma$ -globulin proteins separate the adsorbed albumin film; therefore, the average size of albumin clusters in the contact is lower. This phenomenon causes a greater thickness of lubricating film, which causes lower CoF values; this

deduction is supported by [46]. The lubricant represented by albumin +  $\gamma$ -globulin + HA shows the best frictional properties and the shape area in the resulting graph is the lowest. As was mentioned in the review, HA is very important for ensuring low values of CoF, and it creates the gel-like layer on the AC surface [5], [23], [25], [46]. This layer is very important in prevention of damage, and it is strongly hydrophilic [21], [23]. These properties allow a better adsorption of the protein components contained in the lubricant on the AC surface, which corresponds with the largest amount of protein clusters in the contact. Although the particle count (albumin clusters) is the highest, the increase in trend of lubricating film area is slow. The area of the shape in resulting graph is the smallest, which points to high stability of created lubricating film. Albumin binds to  $\gamma$ -globulin, and then is adsorbed on HA gel-like layer. The AC structure is well protected from damage, and a thick protein film is created, which allows rapid reduction of CoF. The HA contained in the lubricant acts as a stabilizer. Complex model synovial fluid containing all basic components (albumin +  $\gamma$ -globulin + HA + phospholipids) gives a slightly higher values of CoF and lower area of lubricating film than the previous lubricant. This composition of the lubricant is the only one with constantly raising trend of lubricating film area; this phenomenon wasn't observed in any configuration. The rising trend of lubricating film area indicates stability, which allows complete protection of the AC surface for a longer period of time. Phospholipids are bonded to the HA by phosphate cores and to other phospholipids by lipid tails, which is the basis of hydration lubrication [22]. This model assures two phospholipidic layers opposite each other (phospholipidic bilayer) to achieve the hydration model which is not compliant with the model of NSJ used in this thesis. The phospholipids in the lubricant cause the imprisonment of protein clusters between them, which leads to accumulation of protein clusters [46]. This phenomenon is the reason for the increase in the lubricating film area. The higher values of CoF are caused by absence of phospholipidic bilayer. The friction process does not take place between the phospholipidic layers as mentioned in [22]. One layer of phospholipids acts as a brush, which makes the lubricant flowing through the contact difficult. The model of lubricating film formation was published and described in the third study attached to this thesis [31].

## 7 CONCLUSIONS

A healthy NSJ ensures painless human movement with uniquely low friction, thanks to unique tribological properties of the AC. Active life is very important for staying happy and without stress, nevertheless it can be interrupted by many kinds of joint diseases, which can lead to irreversible destruction of the NSJ. This state is often solved by the use of artificial joints. Unfortunately, they have a limited service life, which leads to the necessity of replacing the original artificial joint. If the necessity of replacement with the artificial joint occurs in young age, there is a potential problem with its reoperation, after the service life has elapsed. The general effort is to postpone the necessity of replacement of the NSJ with artificial joint as long as possible, because the human organism is not able to withstand the surgery too many times. The surgery influences the psychological state of the patient and also the subchondral bone degradation occurs. In order to avoid the necessity of replacing the NSJ with artificial joint, scientists discovered viscosupplementation (the supplement based on HA, which is needed to the joint gap). This supplement allows restarting of the lubricating processes of NSJ, which ideally stops the disease progression, or at least slows it down. The same effect of supplements in all patients is not guaranteed, which points to incomplete understanding of NSJ lubricating. Full understanding of lubrication processes in the NSJ allows us to develop effective treatment for all patients with diseased joints.

The research focused on the biotribology of NSJ contains many studies dealing with the frictional properties of the NSJ. Various experimental configurations and their impact to friction properties were observed. It can be said that the frictional behaviour of the AC is described in detail. Studies dealing with the lubrication processes appear a smaller number. The authors observe the impact of composition or experimental conditions on the lubricating film forming, using frictional or optical methods. The theoretical models of lubrication mechanism were developed within these studies, nevertheless, they usually don't have fully experimental background. The visualization of the AC contact is rarely discussed by authors, however, such focused studies do exist. The authors describe the influence of the composition of lubricants on lubrication, and also the impact of concentration of individual components of model SF was observed. The simultaneous contact visualization and friction measurement is discussed very rarely, nevertheless, a few of such focused studies does exist. These studies almost always used the PVA hydrogel instead of AC sample, and the visualization was performed either after the experiments or was not performed continuously. There is no work performing simultaneous AC contact visualization and friction measurements. This thesis fills this white space in this field, which can help us to better understand the lubrication system prevailing in the NSJ, and the gained knowledge can contribute to development of effective treatment of diseased NSJ.

The new evaluation approach of a contact provided by the model of NSJ is introduced in this thesis and using it, the description of lubricating film forming is given. This system of AC contact evaluation has not yet been published. The main conclusions of this thesis can be summarized as follows:

- New evaluating methodology of articular cartilage contact was developed, including a specially designed reciprocating tribometer, evaluation software and experimental data procedure
- Due to the new evaluation methodology of articular cartilage contact, the lubricating film formation in a model of synovial joint was performed, and the impact of individual components using albumin protein observation was described

Regarding the scientific questions, the obtained knowledge can be summarized in the following concluding remarks:

- From the performed investigation, simple albumin solution creates lubricating film with high amount of particles in the contact, however, this film is gradually wiped, which confirm that simple albumin solution does not create stable lubrication film. The lubricant which consists the mixture of albumin and  $\gamma$ -globulin proteins, gives better lubricating and frictional properties, which was expected based on previous studies. The count of albumin clusters in the contact was lower than in the simple albumin solution, which is attributed to the bonding between albumin and  $\gamma$ -globulin. Due to  $\gamma$  globulin protein having bigger size than albumin, the  $\gamma$  globulin surface is covered by albumin proteins, and albumin proteins bind to cartilage surface, optionally to gel-like layer of hyaluronic acid. Hyaluronic acid used in lubricant with mixture of proteins causes significant reduction of friction and the cartilage contact area shows much more particles of albumin. Hyaluronic acid creates the gel like layer on the cartilage surface, and due to high hydrophilicity of hyaluronic acid, the protein adsorption on the cartilage surface (gel-like layer) is more significant. The complex model synovial fluid containing protein components, hyaluronic acid and phospholipids gives higher values of friction than lubricant without phospholipids; however, the lubricating film area increases, which was indicated only for this lubricant composition.

**(HYPOTHESIS WAS NOT FALSIFIED WITHIN THIS THESIS)**

- The best frictional properties were observed for the lubricant with composition of protein components and hyaluronic acid, which was also the lubricant that shows the highest number of particles in the cartilage contact. Nevertheless, the simple albumin solution showed higher particles count in the contact than the mixture of albumin and  $\gamma$ -globulin, which gives better values of friction coefficient.

**(HYPOTHESIS WAS FALSIFIED WITHIN THIS THESIS)**

## REFERENCES

- [1] HAMER, Mark, Romano ENDRIGHI a Lydia POOLE. Physical Activity, Stress Reduction, and Mood: Insight into Immunological Mechanisms. YAN, Qing, ed., Qing YAN. *Psychoneuroimmunology* [online]. Totowa, NJ: Humana Press, 2012, s. 89-102
- [2] BUCKWALTER, J a J MARTIN. Osteoarthritis☆. *Advanced Drug Delivery Reviews* [online]. 2006, **58**(2), 150-167
- [3] ACKERMAN, Ilana, Megan BOHENSKY, Richard DE STEIGER et al. Lifetime Risk of Primary Total Hip Replacement Surgery for Osteoarthritis From 2003 to 2013: A Multinational Analysis Using National Registry Data. *Arthritis Care & Research* [online]. 2017, **69**(11), 1659-1667
- [4] BELLAMY, Nicholas, Jane CAMPBELL, Vivian WELCH, Travis GEE, Robert BOURNE a George WELLS. Viscosupplementation for the treatment of osteoarthritis of the knee. *Cochrane Database of Systematic Reviews*
- [5] REBENDA, David, Martin VRBKA, Pavel ČÍPEK, Evgeniy TOROPITSYN, David NEČAS, Martin PRAVDA a Martin HARTL. On the Dependence of Rheology of Hyaluronic Acid Solutions and Frictional Behavior of Articular Cartilage. *Materials* [online]. 2020, **13**(11), 1-14
- [6] LINK, Jarrett, Evelia SALINAS, Jerry HU a Kyriacos ATHANASIOU. The tribology of cartilage: Mechanisms, experimental techniques, and relevance to translational tissue engineering. *Clinical Biomechanics* [online]. 2020, **79**
- [7] STACHOWIAK, G.W., A.W. BATCHELOR a L.J. GRIFFITHS. Friction and wear changes in synovial joints. *Wear* [online]. 1994, **171**(1-2), 135-142
- [8] CHAN, S.M.T., C.P. NEU, K. KOMVOPOULOS a A.H. REDDI. The role of lubricant entrapment at biological interfaces: Reduction of friction and adhesion in articular cartilage. *Journal of Biomechanics* [online]. 2011, **44**(11), 2015-2020
- [9] ALMARZA, Alejandro a Kyriacos ATHANASIOU. Design Characteristics for the Tissue Engineering of Cartilaginous Tissues. *Annals of Biomedical Engineering* [online]. 2004, **32**(1), 2-17
- [10] MOORE, Axel a David BURRIS. New Insights Into Joint Lubrication. *Tribology & Lubrication Technology* [online]. 2016, **72**(5), 26-30
- [11] GREENE, George, Bruno ZAPPONE, Boxin ZHAO, Olle SÖDERMAN, Daniel TOPGAARD, Gabriel RATA a Jacob ISRAELACHVILI. Changes in pore morphology and fluid transport in compressed articular cartilage and the implications for joint lubrication. *Biomaterials* [online]. 2008, **29**(33), 4455-4462
- [12] POOLE, A, I PIDOUX, A REINER a L ROSENBERG. An immunoelectron microscope study of the organization of proteoglycan monomer, link protein, and collagen in the matrix of articular cartilage. *Journal of Cell Biology* [online]. 1982, **93**(3), 921-937
- [13] MOW, Van, Mark HOLMES a W. MICHAEL LAI. Fluid transport and mechanical properties of articular cartilage: A review. *Journal of Biomechanics* [online]. 1984, **17**(5), 377-394



- [14] CHEN, A.C., W.C. BAE, R.M. SCHINAGL a R.L. SAH. Depth- and strain-dependent mechanical and electromechanical properties of full-thickness bovine articular cartilage in confined compression. *Journal of Biomechanics* [online]. 2001, **34**(1), 1-12
- [15] GLEGHORN, Jason a Lawrence BONASSAR. Lubrication mode analysis of articular cartilage using Stribeck surfaces. *Journal of Biomechanics* [online]. Elsevier Ltd, 2008, **41**(9), 1910-1918
- [16] ACCARDI, Mario, Daniele DINI a Philippa CANN. Experimental and numerical investigation of the behaviour of articular cartilage under shear loading—Interstitial fluid pressurisation and lubrication mechanisms. *Tribology International* [online]. 2011, **44**(5), 565-578
- [17] MCCUTCHEN, C.W. The frictional properties of animal joints. *Wear* [online]. 1962, **5**(1), 1-17
- [18] WALKER, P, D DOWSON, M LONGFIELD a V WRIGHT. "Boosted lubrication" in synovial joints by fluid entrapment and enrichment. *Annals of the Rheumatic Diseases* [online]. 1968, **27**(6), 512-520
- [19] MANSOUR, Joseph a Van MOW. On the Natural Lubrication of Synovial Joints: Normal and Degenerate. *Journal of Lubrication Technology* [online]. 1977, **99**(2), 163-172
- [20] SWANN, D.A., H.S. SLAYTER a F.H. SILVER. The molecular structure of lubricating glycoprotein-I, the boundary lubricant for articular cartilage. *Journal of Biological Chemistry* [online]. 1981, **256**(11), 5921-5925
- [21] MURAKAMI, Teruo, Seido YARIMITSU, Nobuo SAKAI, Kazuhiro NAKASHIMA, Tetsuo YAMAGUCHI a Yoshinori SAWAE. Importance of adaptive multimode lubrication mechanism in natural synovial joints. *Tribology International* [online]. 2017, **113**, 306-315
- [22] JAHN, Sabrina, Jasmine SEROR a Jacob KLEIN. Lubrication of Articular Cartilage. *Annual Review of Biomedical Engineering* [online]. 2016, **18**(1), 235-258
- [23] FORSEY, R, J FISHER, J THOMPSON, M STONE, C BELL a E INGHAM. The effect of hyaluronic acid and phospholipid based lubricants on friction within a human cartilage damage model. *Biomaterials* [online]. 2006, **27**(26), 4581-4590
- [24] MURAKAMI, T, K NAKASHIMA, Y SAWAE, N SAKAI a N HOSODA. Roles of adsorbed film and gel layer in hydration lubrication for articular cartilage. *Proceedings of the Institution of Mechanical Engineers, Part J: Journal of Engineering Tribology* [online]. 2009, **223**(3), 287-295
- [25] HIGAKI, H, T MURAKAMI, Y NAKANISHI, H MIURA, T MAWATARI a Y IWAMOTO. The lubricating ability of biomembrane models with dipalmitoyl phosphatidylcholine and  $\gamma$ -globulin. *Proceedings of the Institution of Mechanical Engineers, Part H: Journal of Engineering in Medicine* [online]. 1998, **212**(5), 337-346
- [26] YARIMITSU, Seido, Kazuhiro NAKASHIMA, Yoshinori SAWAE a Teruo MURAKAMI. Influences of lubricant composition on forming boundary film composed of synovia constituents. *Tribology International* [online]. 2009, **42**(11-12), 1615-1623

- [27] YARIMITSU, Seido, Kazuhiro NAKASHIMA, Yoshinori SAWAE a Teruo MURAKAMI. Effects of Lubricant Composition on Adsorption Behavior of Proteins on Rubbing Surface and Stability of Protein Boundary Film. *Tribology Online* [online]. 2008, **3**(4), 238-242
- [28] NAKASHIMA, K., Y. SAWAE a T. MURAKAMI. Study on wear reduction mechanisms of artificial cartilage by synergistic protein boundary film formation. *JSME International Journal, Series C: Mechanical Systems, Machine Elements and Manufacturing* [online]. 2006, **48**(4), 555-561
- [29] ČÍPEK, Pavel, David REBENDA, David NEČAS, Martin VRBKA, Ivan KŘUPKA a Martin HARTL. Visualization of Lubrication Film in Model of Synovial Joint. *Tribology in Industry* [online]. 2019, **41**(3), 387-393
- [30] ČÍPEK, Pavel, Martin VRBKA, David REBENDA, David NEČAS a Ivan KŘUPKA. Biotribology of Synovial Cartilage: A New Method for Visualization of Lubricating Film and Simultaneous Measurement of the Friction Coefficient. *Materials* [online]. 2020, **13**(9), 1-19
- [31] PAVEL, Čípek, Martin VRBKA, David REBENDA, David NEČAS a Ivan KŘUPKA. Biotribology of Synovial Cartilage: Role of Albumin in Film Formation. *Engineering Science and Technology, an International Journal*. **2022**, 0-12. ISSN 22150986.
- [32] NEČAS, D., M. VRBKA, A. GALANDÁKOVÁ, I. KŘUPKA a M. HARTL. On the observation of lubrication mechanisms within hip joint replacements. Part I: Hard-on-soft bearing pairs. *Journal of the Mechanical Behavior of Biomedical Materials* [online]. 2019, **89**, 237-248
- [33] HODGE, W., R. FIJAN, K. CARLSON, R. BURGESS, W. HARRIS a R. MANN. Contact pressures in the human hip joint measured in vivo. *Proceedings of the National Academy of Sciences* [online]. 1986, **83**(9), 2879-2883
- [34] LAKOWICZ, Joseph R. *Principles of fluorescence spectroscopy*. 3rd ed. New York: Springer, 2006. ISBN 978-0-387-31278-1.
- [35] CILINGIR, Ahmet C. Effect of rotational and sliding motions on friction and degeneration of articular cartilage under dry and wet friction. *Journal of Bionic Engineering* [online]. 2015, **12**(3), 464-472
- [36] PICKARD, J.E., J. FISHER, E. INGHAM a J. EGAN. Investigation into the effects of proteins and lipids on the frictional properties of articular cartilage. *Biomaterials* [online]. 1998, **19**(19), 1807-1812
- [37] FITZGERALD, Jonathan, Moonsoo JIN a Alan GRODZINSKY. Shear and Compression Differentially Regulate Clusters of Functionally Related Temporal Transcription Patterns in Cartilage Tissue. *Journal of Biological Chemistry* [online]. 2006, **281**(34), 24095-24103
- [38] MOW, V., S. KUEI, W. LAI a C. ARMSTRONG. Biphasic Creep and Stress Relaxation of Articular Cartilage in Compression: Theory and Experiments. *Journal of Biomechanical Engineering* [online]. 1980, **102**(1), 73-84

- [39] ACHARYA, Tinku a Ajoy RAY. *Image Processing: Principles and Applications*. 1. NJ: John Wiley: Hoboken, 2005. ISBN 978-0-471-71998-4.
- [40] VINCENT, Luc. Morphological Area Openings and Closings for Grey-scale Images. O, Ying-Lie, Alexander TOET, David FOSTER, Henk J. A. M. HEIJMANS a Peter MEER, ed., Ying-Lie O, Alexander TOET, David FOSTER, Henk HEIJMANS, Peter MEER. *Shape in Picture* [online]. 126. Berlin, Heidelberg: Springer Berlin Heidelberg, 1994, s. 197-208
- [41] RADIN, ERIC, DAVID SWANN a PAUL WEISSER. Separation of a Hyaluronate-free Lubricating Fraction from Synovial Fluid. *Nature* [online]. 1970, **228**(5269), 377-378
- [42] MOW, Van, Anthony RATCLIFFE a A. ROBIN POOLE. Cartilage and diarthrodial joints as paradigms for hierarchical materials and structures. *Biomaterials* [online]. 1992, **13**(2), 67-97
- [43] JEYACHANDRAN, Y., E. MIELCZARSKI, B. RAI a J. MIELCZARSKI. Quantitative and Qualitative Evaluation of Adsorption/Desorption of Bovine Serum Albumin on Hydrophilic and Hydrophobic Surfaces. *Langmuir* [online]. 2009, **25**(19), 11614–11620
- [44] WU, Ting-ting, Xue-qi GAN, Zhen-bing CAI, Min-hao ZHU, Meng-ting QIAO a Haiyang YU. The lubrication effect of hyaluronic acid and chondroitin sulfate on the natural temporomandibular cartilage under torsional fretting wear. *Lubrication Science* [online]. 2015, **27**(1), 29-44
- [45] NEČAS, David, Martin VRBKA, Filip URBAN, Ivan KŘUPKA a Martin HARTL. The effect of lubricant constituents on lubrication mechanisms in hip joint replacements. *Journal of the Mechanical Behavior of Biomedical Materials* [online]. 2016, **55**, 295-307
- [46] FURMANN, Denis, David NEČAS, David REBENDA, Pavel ČÍPEK, Martin VRBKA, Ivan KŘUPKA a Martin HARTL. The Effect of Synovial Fluid Composition, Speed and Load on Frictional Behaviour of Articular Cartilage. *Materials* [online]. 2020, **13**(6)

## AUTHOR'S PUBLICATIONS

### JOURNALS

ČÍPEK, P.; VRBKA, M.; REBENDA, D.; NEČAS, D.; KŘUPKA, I. Biotribology of Synovial Cartilage: A New Method for Visualization of Lubricating Film and Simultaneous Measurement of the Friction Coefficient. *Materials*, 2020, roč. 13, č. 9, s. 1-20. ISSN: 1996-1944.

REBENDA, D.; VRBKA, M.; ČÍPEK, P.; TOROPITSYN, E.; NEČAS, D.; PRAVDA, M.; HARTL, M. On the Dependence of Rheology of Hyaluronic Acid Solutions and Frictional Behavior of Articular Cartilage. *Materials*, 2020, roč. 13, č. 11, s. 1-14. ISSN: 1996-1944.

FURMANN, D.; NEČAS, D.; REBENDA, D.; ČÍPEK, P.; VRBKA, M.; KŘUPKA, I.; HARTL, M. The effect of synovial fluid composition, speed and load on frictional behaviour of articular cartilage. *Materials*, 2020, roč. 13, č. 6, s. 1-16. ISSN: 1996-1944.

ČÍPEK, P.; REBENDA, D.; NEČAS, D.; VRBKA, M.; KŘUPKA, I.; HARTL, M. Visualization of Lubrication Film in Model of Synovial Joint. *Tribology in Industry*, 2019, roč. 41, č. 3, s. 387-393. ISSN: 0354-8996.

ČÍPEK, P.; VRBKA, M.; REBENDA, D.; NEČAS, D.; KŘUPKA, I. Biotribology of Synovial Cartilage: Role of Albumin in Adsorbed Film Formation. *Engineering Science and Technology, an International Journal*. 2022, 34, 101090. ISSN: 22150986

### CONFERENCE ABSTRACTS AND PROCEEDINGS

ČÍPEK, P.; REBENDA, D.; VRBKA, M.; HARTL, M. OBSERVATION OF LUBRICATION FILM IN SYNOVIAL JOINT. In *Proceedings on Engineering Science. Proceedings on Engineering Sciences - 16th International Conference on Tribology*. Kragujevac: University of Kragujevac, Faculty of Engineering, 2019. s. 687-692. ISSN: 2620-2832.

REBENDA, D.; ČÍPEK, P.; VRBKA, M.; KŘUPKA, I. Effect of Hyaluronic Acid Molecular Weight on Friction of Articular Cartilage. In *Proceedings on Engineering Sciences - 16th International Conference on Tribology. Proceedings on Engineering Sciences - 16th International Conference on Tribology*. Kragujevac: University of Kragujevac, Faculty of Engineering, 2019. s. 693-697. ISSN: 2620-2832.

ČÍPEK, P.; REBENDA, D.; NEČAS, D.; VRBKA, M.; KŘUPKA, I. Development of reciprocating tribometer for testing synovial joint. In *Engineering Mechanics 2018. Engineering Mechanics 2018*. First edition. Praha: Institute of Theoretical and Applied Mechanics of the Czech Academy of Sciences, Prague, 2018. s. 169-172. ISBN: 978-80-86246-88-8. ISSN: 1805-8256.

REBENDA, D.; ČÍPEK, P.; NEČAS, D.; VRBKA, M.; HARTL, M. Effect of Hyaluronic Acid on Friction of Articular Cartilage. In *Engineering Mechanics 2018*. First. Praha: Institute of Theoretical and Applied Mechanics of the Czech Academy of Sciences, 2018. s. 709-712. ISBN: 978-80-86246-91-8.

# CURRICULUM VITAE

Ing. Pavel Čípek

Date and place of birth: 11/03/1992, Brno

## Education

- **2016 – 2021** Doctoral study at Institute of Machine and Industrial Design, Faculty of Mechanical Engineering, Brno University of Technology. Topic of the dissertation thesis: *The Effect of Synovial Fluid Constituents on Friction and Lubrication of Articular Cartilage*.
- **2014 – 2016** Master study at Institute of Machine and Industrial Design, Faculty of Mechanical Engineering, Brno University of Technology. Topic of the diploma thesis: *Testing of Automotive Sport Suspension*.
- **2011 – 2014** Bachelor study at Faculty of Mechanical Engineering, Brno University of Technology. Topic of the bachelor thesis: *Design of Equipment for Excitation of Vibrations*.
- **2007 – 2011** Secondary Industrial School, Jedovnice. Branch: Engineering.

## Teaching activities – seminars:

- Machine design – Machine Elements (5KS)
- Machine design – Mechanical Drives (6KT)
- Mechanical Design Project (ZIP)
- Team project (ZKP)
- Tribology (ZTR)

## Participations in scientific projects

- 2020 – 2022: Study of tribological properties of small joint replacements (FSI-S-20-6443).
- 2018: Innovation of subject teaching of tribology through employ of visualization of contact of synovial joint. (FV 18-26)
- 2017 – 2019: Study of the influence of lubricant rheology in elastohydrodynamically lubricated contacts (FSI-S-17-4415).

## Language skills

Czech, English (B2)

## Scientific activities

- Biotribology – lubricating in synovial joints

## **ABSTRACT**

The present PhD thesis deals with the lubricating mechanism within a model of synovial joint. The aim of this thesis is to describe the effect of individual components of synovial fluid on lubricating film formation in the model of synovial joint; for this purpose, the experimental analysis of friction coefficient and observation of adsorbed lubricating film using the fluorescence microscopy were performed. The special self-designed reciprocating tribometer allowing for simultaneous friction measurement and contact observation was designed. The tribometer was calibrated and verified using a commercial tribometer. Furthermore, the methodology of experiments was developed including a design of evaluation procedure. In order to process the visualization record, the software based on the image segmentation was developed. The last part of the thesis introduces a novel methodological approach together with a new self-designed tribometer enabling to assess the role of components contained in the model synovial fluid in relation to the formation of lubricating film based on in situ observation of the contact area and simultaneous frictional measurement. The thesis presents original results extending the knowledge in the natural synovial joint biotribology towards the further development of effective treatment for patients with diseased joints.

## **ABSTRAKT**

Práce se zabývá problematikou biotribologie modelu synoviálního kloubu. Cílem práce je popsat vliv složek synoviální kapaliny na formování mazacího filmu v modelu synoviálního kloubu. Práce je zaměřena na experimentální analýzu součinitele smykového tření a jeho propojení s pozorováním adsorbovaného mazacího filmu v kontaktu pomocí fluorescenční mikroskopie. Součástí práce je návrh tribometru, který umožňuje vizualizaci v průběhu experimentů. Tribometr je vyroben, kalibrován a verifikován pomocí komerčního tribometru. Dále je součástí práce návrh metodiky experimentů včetně návrhu postupu pro zpracování a hodnocení výsledků. Pro zpracování záznamu z vizualizace kontaktu byl navržen speciální software, který pracuje na principu segmentace obrazu. Poslední část práce je zaměřena na aplikaci vyvinuté metodologie spolu s nově navrženým tribometrem, což umožňuje posoudit roli složek modelové kapaliny u formování mazacího filmu v modelu synoviálního kloubu. Experimentální část je založena na měření tření za současné vizualizace kontaktu. Tato práce prezentuje originální výsledky rozšiřující oblast biotribologie synoviálního kloubu, které mohou pomoci dalšímu rozvoji účinné léčby pacientů s nemocnými klouby.